Scanning Microscopy

Volume 2 | Number 3 Article 10

2-6-1988

Metal Ion and Cluster Beams for Microelectronic Research and Development: A Review

G. Ben Assayag
Laboratoire L2M-CNRS

P. Sudraud
Laboratoire L2M-CNRS

Follow this and additional works at: https://digitalcommons.usu.edu/microscopy

 Part of the Biology Commons

Recommended Citation

Assayag, G. Ben and Sudraud, P. (1988) "Metal Ion and Cluster Beams for Microelectronic Research and Development: A Review," *Scanning Microscopy*: Vol. 2 : No. 3 , Article 10.
Available at: https://digitalcommons.usu.edu/microscopy/vol2/iss3/10

This Article is brought to you for free and open access by the Western Dairy Center at DigitalCommons@USU. It has been accepted for inclusion in Scanning Microscopy by an authorized administrator of DigitalCommons@USU. For more information, please contact digitalcommons@usu.edu.

Scanning Microscopy, Vol. 2, No. 3, 1988 (Pages 1329-1341) 0891-7035/88$3.00+.00
Scanning Microscopy International, Chicago (AMF O'Hare), IL 60666 USA

METAL ION AND CLUSTER BEAMS FOR MICROELECTRONIC RESEARCH AND DEVELOPMENT : A REVIEW

G. BEN ASSAYAG*, P. SUDRAUD

LABORATOIRE L2M-CNRS
196 A. H. RAVERA
92220-BAGNEUX-FRANCE

(Received for publication May 05, 1987, and in revised form February 06, 1988)

Abstract

Applications of focused ion and cluster beams emitted by liquid metal ion sources are particularly attractive in microelectronic engineering. We overview this area of research and development adding recent results concerning repair, tuning and characterization obtained either by focusing ions or droplets on a microcircuit controlled by in-situ SEM observation of the process.

Key Words: Liquid metal ion source, Scanning ion microscopy, microlithography, localized implantation, focused droplet beams, focused ion beams.

***Address for correspondence:**
G. Ben Assayag, Laboratoire L2M-CNRS
196 Avenue H. Ravera
92220-Bagneux-France
Phone No:(1) 45-29-55-03

Introduction

In 1973, Seliger and Fleming investigated for the first time the potential applications of focused ion beams in microelectronics; they mentioned doping, damage in crystal structures, molecular bond breaking. They said : " The objective is to demonstrate unique microfabrication techniques such as maskless implantation doping and the formation of self-aligned structures".

In 1987, focused ion beam systems have an increasing number of applications in microlithography, micromachining, high resolution secondary ion mass spectrometry, localized implantation or more recently localized metal deposition. These systems usually provide 0.1-0.2µm ion probes of a number of species (Ga, Si, Be, B, As, Sn ...) with a current density of $1A/cm^2$.

If one considers a given area of a solid (a part of a wafer for example) to be physically or chemically modified by ion beam irradiation, the time necessary to treat a unit surface depends only on total dose governed by total current.

When focusing a particle beam into a probe, the optical aberration effects make it necessary to reduce the beam aperture to values of the order of a milliradian.

The result is a dramatic decrease in the probe current and a subsequent increase of the treatment time per unit area.

The limited brightness of classical ion sources (duoplasmatrons, etc...) limits the value of the current at typical values of 0.6pA for a 300 nm diameter probe leading to prohibitive times for microfabrication.

During the 70's, the advent of liquid metal ion sources boosted the attainable current values for a given probe size by several orders of magnitude, making the original ideas of Seliger and Fleming feasible.

Ion - Solid Interaction

Generalities

The impact of primary ions I on a surface II induces various secondary effects. Each one has potential applications in physics, microelectronics, microanalysis, solid modification, etc..

The effect of ion irradiation and its corresponding application are summarized in the following Table 1.

Most of the techniques have thus far been developed for microelectronics engineering, using large, or poorly focused beams. The advent of submicronic ion probes further widened this impressive domain of applications, providing the unique possibility of very localized modification of a solid.

The two main processes involved in present focused ion beam applications are ion sputtering and implantation. We overview the principal characteristics of both phenomena.

Sputtering

A surface irradiated by energetic particles is eroded by the removal of surface atoms. Sigmund (1981) showed that the sputtering yield of metals, which is the number of removed atoms per incident ion, depends on primary particle energy and mass, mass of the target atoms, incidence angle, residual gas pressure, crystal orientation. Below a threshold energy which is about 20 to 40 eV for normal incidence, no sputtering occurs. Above this threshold, the yield increases with incident energy and reaches a broad maximum in the energy region of 5 to 50 keV. At oblique angle of ion bombardment the sputtering yield increases monotonically with increasing angle up to 70 to 80°. Higher mass particles gives mostly larger sputtering yields than lighter ions. For example, from Andersen and Bay (1981), a maximum sputtering yield of 2 atoms per Ar incident ion is measured at 20keV for a silicon target. At 100 kV this value decreases and is lower than 1. With a 19 keV Ga FIB, we have measured on a silicon target a sputtering yield of 3.3 atoms per ion. This yield can be improved by gas assisted etching using a reactive gas such as chlorine. Ochiai et al. (1984) mentioned a yield increase of a factor of 8. The domain of some tens of keV for heavy species is well adapted to the focusing of submicron probes for machining applications.

Implantation

Ion implantation is conceptually one of the simplest methods for modifying particular properties of a semiconductor in selected regions. The problem is to decide which electrical, physical, optical or mechanical properties are required and to choose the chemical composition to achieve these results. Maskless focused ion beam implantation (FIBI) offers the possibility of simplifying local modification of electronic properties in a solid. So, FIBI can be considered as a submicron tool for localized gap modification. The penetration depth is a function of the atomic mass of both incident ion and target and increases with the energy of the primary beam. Table 2 shows calculated values of the projected range R_p in GaAs.

To reach a reasonable penetration depth in semiconductors for p and n dopants (of the order of 0.1μm) a minimum energy of some hundreds of keV is necessary, except for the lighter elements such as B or Be.

The creation of crystal defects and irradiation damages disturbs the electrical properties of devices. A subsequent thermal annealing is usually necessary to restore crystal structure. Available theories (Townsend et al (1976)) of irradiation damage are not completely satisfactory for FIBI. Energy deposited by submicron ion probes induces a local elevation of temperature which may affect the extent of lateral diffusion.

Finally, two energy ranges emerge as relevant from the characteristics of sputtering and implantation processes :

E = 10 keV range for maximum machining efficiency.

E = 100 keV range for reasonable penetration depth in ion implantation.

Focused Ion Beam Machines

Principle of liquid metal ion sources

As mentioned above, the development of practical focused ion beam machines has been made possible by the advent of liquid metal ion sources (LMIS). The liquid metal emitter was originally studied, in the seventies, by several authors including Krohn (1961), Krohn and Ringo (1975), Mahoney et al (1969), Clampitt et al (1975). The early developments of these electrohydrodynamic emitters were directed at electric space propulsion purposes.

In an operating LMIS a liquid metal flows onto a tungsten needle up to a sharp apex. When a critical positive voltage is applied between the ion source and an extractor, an ion current from 1 to 100 μA is available. The emission appears at the apex of a liquid conical structure described by Taylor (1964) and more recently by the group of Cutler et al (1986) and by Swanson and Kingham (1986). In-situ high voltage TEM pictures of an operationg LMIS shows that the extreme apex of the liquid exhibits a distorted cone shape, with concave walls (cusp). A fine jet-like protusion terminates the structure (Ben Assayag et al. 1985, Gaubi et al. 1982) and its size is about 1.5 nm radius at 10μA emission current. The virtual source size is much

Table 1 : The effects of ion irradiation and its applications.

SECONDARY EMISSION	APPLICATION
scattered ions I	Rutherford backscattering
secondary ions I-II	SIMS, SNMS
Secondary neutrals I-II	Machining, post-ionization SIMS
photons	IIXE
secondary electrons	SIM
SURFACE EFFECTS	
dislocations	electrical isolation
chemical sputtering	repair, machining
physical sputtering	repair, machining
secondary ions	scanning ion microscopy, SIMS
assisted chemical deposition	device repair
cluster deposition	metal deposition
BULK PHENOMENA	
volume dislocations	electrical isolation
molecular bond breaking	lithography
amorphisation	isolation
implantation	p,n doping or isolation
channeling	ion litho. masks technology

Table 2 : R_p standard projected range for different dopant species in GaAs (Wilson and Brewer 1979).

R_p nm	Be^+	B^+	Ga^+	Si^+
10kV	28	28	8	11
100kV	500	500	32	80

larger and is estimated to be 30 to 50 nm (Komuro et al 1983). The corresponding brightness is about $10^5 A/cm^2$ which is at least 100 times higher than that of other sources. At low emission currents (a few μA), the emission process generally considered is field evaporation of the metal (Gomer 1979). One can expect a very narrow energy spread of the ions (less than 1eV for field ionization on solid surfaces); unfortunately the measured values are about 5 to 10 eV (Ohana R. 1980, Gesley and Swanson 1984) near onset, and increase with current. The subsequent chromatic aberrations suggests that one should work at low current for high resolution, as shown by Fox et al (1981), Mair and Mulvey (1985). The emission stability is also very sensitive to the vacuum quality, and the liquid perturbations due to backscattered secondary atoms, ions or electrons which induce cracking processes and carbonaceous deposition on the emitter (Sudraud et al 1986). A high vacuum (10^{-8} to 10^{-7} torr) is necessary for proper gun operation.

LMIS become more and more reliable. The tip-filament-crucible design initially created in Orsay (Sudraud 1979) has been universally adopted and improved. We currently observe life times of several months for Ga or In LMIS.

The basic concept of LMIS excludes the direct ionization of high vapor pressure and substrate-corrosive elements. Low vapor pressure alloys overcome these problems, (Bozack et al. 1985). A large series of alloys have been developed for impurity-doping of semiconductors. Table 3 summarizes the ion species and corresponding liquid metals :

Table 3 : The different ion species and the corresponding alloyed liquid metal ion source.

ION SPECIES	LIQUID METAL
Ag	Ag
Al	Al
As	Pd-Ni-B-As, As-Sn-Pd, As-Pt
Au	Au
B	Pt-B, Pd-Ni-B, Pt-Ni-B
Be	Au-Be, Au-Si-Be, Ga-Si-Be, Pd-Ni-Si-Be-B
Bi	Bi
Cu	Cu
Cs	Cs
Ga	Ga
Ge	B-Pt-Au-Ge
In	In
Ni	Pd-Ni-B
P	Cu-P
Pb	Sb-Pb-Au
Pd	Pd-Ni-B
Pt	Pt-B
Sb	Sb-Pb-Au
Si	Si, Au-Si, Ga-Si-Be
Sn	Sn, As-Sn-Pd
U	U
Zn	Zn, Zn-Ga

In addition to providing singly and doubly charged particles, liquid metal ion sources emit charged clusters and droplets at high current emission conditions (I=30 to 300 μA). Then, the ability to sputter using the ion mode and deposit metal in the droplet mode in the same apparatus might be an extremely in-

teresting extension of the applications for sytems using LMI sources.

A typical focused ion beam machine

The ultimate aim of an FIB design is to obtain the finest probe for the highest current in order to minimize the working time.

A focused ion beam system is both a masker and an ion implanter. We will distingish the optical column (implanter part) from the more classical object chamber (masker part) . The degree of sophistication of each one can vary widely for different applications.

The focused ion beam systems commercially available have a large range of energy and complexity corresponding to three main domains : sputtering for repairing or modifying devices, microanalysis (SIMS) (10 keV energy range), lithography or implantation (100 keV energy range).

Presently, all existing LMIS systems designed for lithography and implantation use a series of lenses in order to form a critically focused image of the source on the target plane. The spatial current distribution of the probe is roughly gaussian as a consequence of the LMIS emission characteristics.

-The optical column Figure 1 represents a typical FIB column (JEOL).

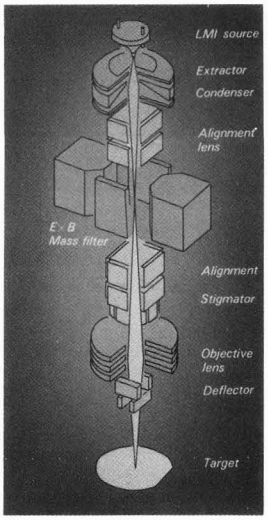

Figure 1 - Principle of a focused ion beam machine (after JEOL).

The ion beam is extracted from an LMIS, focused by condenser and objective electrostatic lenses. A deflector scans the beam on the target. An ExB filter selects ion species when an alloyed metal LMIS is used. Apertures define lens acceptance angles and filter spatial selection.

This concept of column typically allows focusing of a 50 to 200 nm spot carrying a current density of about 1 A/cm2 with pure metal sources. Filtering, in the case of alloyed metals, reduces probe current density depending on the abundance of the doping element in the mass spectrum. For example, compared with Ga, a B probe current density falls by more than one order of magnitude. An effort in the metallurgy of alloys LMIS should be carried out to overcome this problem (Bozack et al. 1985). A number of research efforts are in progress to improve resolution, current density and energy (Shiokawa et al. (1985)) of FIB columns. Electrostatic lenses were employed at the early beginning of electron microscopy in the forties, before being supplanted by magnetic lenses. FIB systems, with the necessity of having charge/mass independent focusing properties, renewed the interest for electrostatic lens calculation programs to optimize their properties (Munro 1973). Due to the LMIS high energy dispersion, the chromatic aberration coefficient is the principal enemy of FIB lenses (Mair and Mulvey 1984). Mass filter aberrations reduction is obtained in the JEOL system by forming a cross-over at the center of the filter. Cleaver et al. (1983) designed a magnetic omega-shaped filter of very low aberration. One advantage of the ExB filter is to allow fast mass switch by adjusting only an electric field.

The positioning of double deflection systems before the last objective lens reduces working distance and corresponding chromatic aberration. Multipolar electrodes have been designed to enlarge the scanned field without distorsion Moriya et al (1983).

-The experiment chamber The experiment chamber which uses either classical or UH vacuum technology for III-V compounds, can include accurate laser interferometry tables and sophisticated softwares very similar to those of maskers or nanomaskers for nanostructures drawings.

Slingerland (1984) and Orloff and Sudraud (1985) have proposed a Köehler illumination system by analogy with Köehler illumination e-beam lithography. These have the advantage of uniform current density delivered onto the target and of overcoming the problem of stochastic 0.3 mrad angular dispersion of LMIS ion trajectories due to coulombian interactions as explained by Ward (1985).

The Applications of Focused Ion Beam

Localized implantation

The use of FIB simplifies the fabrication process by avoiding most masking/lithography steps, and allowing a quick switch of dopant species. Doping profiles can easily be controlled and changed in X, Y and Z directions by software. Unfortunately, the theoretical

resolution of FIBI is limited by lateral straggling of the dopant, due both to collisional cascades during ion irradiation, and to impurity diffusion during the annealing process.

Broad ion beam implantation mechanisms have been modeled with reasonable agreement with experimental observations. Nevertheless considerable doubts remain about the focused ion beam cases where the current density is much higher than in classical implantation. One can expect a substantial increase of local temperature and subsequent modification of crystal defects concentration, diffusion and lateral spread of impurities. Some authors have also reported evidence of self-annealing processes which can restore the crystal.

Despite an ion spot having a diameter of 0.1μm, Miyauchi et al. (1983) measured for high implantation dose ($5x10^{14}$ cm^{-2}) up to 1μm or more lateral spread of 160kV-implanted Si or Be into GaAs. However, they conclude that doping of submicron width can be realized with low doses or shallow implantation.

The interesting approach of Reuss et al. (1985) is to compare the results of the fabrication of the same device with conventional and FIB (75kV, 30 mA/cm^2) B implants. Electrical measurements on two vertical npn bipolar transistors fabricated on the same wafer with conventional and focused ion implantation are comparable. They demonstrate fabrication of transistors with lateral doping profiles to reduce crowding and base resistance.

The formation of isolation regions has also been demonstrated using boron or gallium implantation. Nakamura et al. (1987) formed highly resistive region by Ga focused ion beam single line implantation. This submicron (0.4μm) isolation region can be formed in n-GaAs layers with the conductive layer carrier concentration up to $1x10^{18}$ cm^{-3}. The high resistivity $2x10^4$ Ω cm was stable up to 900 °C annealing temperature. Such a high resistivity was not observed in p-GaAs regions. Similar results were obtained using a Ga unfocused ion beam.

Submicron isolation in GaAs was also performed by using boron ions from a complex alloyed LMIS Pd-Ni-Si-Be-B. H. Arimoto et al. (1985) report a resistivity of 10^4 to 10^5 Ω cm with less than 0.5μm line width after 100kV boron implantation in n-GaAs $2x10^{17}/cm^3$. 800 °C annealing did not modify the insulating properties.

For a variety of high-speed electronic and optoelectronic devices and their integrated circuits the crystal growth by molecular beam epitaxy (MBE) of heterostructures in III-V compounds is suitable. These devices have complicated structures and numerous fabrication steps including an alternation of crystal growth and ion implantation. But growing high quality epitaxial layers on air exposed surface is difficult. In classical implantation, the wafer is encapsulated to avoid surface oxidation and impurities adsorption during the tranfer. Miyauchi and Hashimoto (1986) have built an FIB implanter-MBE crystal growth system with a constant minimum vacuum of $5x10^{-9}$ Torr. Crystal growth and ion implantation of Be and Si have been done alternatively to superimpose p (80kV Be) and n (160kV Si) submicron doped lines in multilayer structures. Multilayered crystals with three dimensional arbitrary pattern-doped regions of submicron size were grown using computer software without any air exposure (Hashimoto et al. 1986). The carrier profile in air exposed and non-exposed regrowth interface was measured which demonstrates no carrier depletion in the non-exposed crystal.

Ishida et al. (1986) fabricated buried optical guide (BOG) in GaAs. The principle is based on the fact that the compositional disordering of Si doped multiquantum well is suppressed by Be ion implantation and subsequent annealing. Their process is completely planar and very simple. Despite a high value of threshold current, the tranverse mode MQW-BOG fabricated is a first step for designing optoelectronic integrated microdevices. Compositional disordering of a Ga FIB implanted GaAs/GaAlAs superlattice during post-implantation annealing has been shown by Hirayama et al. (1985). Low temperature cathodoluminescence topography shows that a submicron periodic structure of the superlattice and the mixed crystal was fabricated.

These developments illustrate the power of coupled FIBI-MBE systems for research in integrated optoelectronics fabrication. A serious effort for a better physical understanding of FIB/solid interaction is necessary to minimize lateral straggling and to establish the absolute lateral resolution limit for FIBI.

Microlithography

Ion beam lithography is a new potential means for producing electronic devices with submicron dimensions. In recent years, much work concerned masked ion beam lithography (Pang et al. 1987) with broad beams irradiation.

Electron beam lithography is more developed because technological means for obtaining a fine focused electron spot are well-known. But it involves several problems such as low resist sensitivity, proximity effects and backscattering from the surface.

Ion beam lithography overcomes most of these problems. First, resist exposure sensitivity is one or two orders of magnitude higher for ions than electrons (Karapiperis et al. 1985). There is ne-

gligible ion scattering in the resist (Karapiperis et al. 1981). Backscattered electrons from the substrate have low energy. Therefore, except ion straggling, the structures are practically defined by the primary ion beam.

Most of the reports on ion beam lithography have involved broad beams where light ions H^+, He^+ or B^+ are used. At 100kV the penetration depth of these ions reaches 1µm. For FIB systems using intense and reliable liquid metal ion sources such as Ga, Au, Sn the penetration depth is very small. For Ga and 100kV acceleration voltage 0.1µm is typical.

Precise characteristics of resists were studied by Matsui et al. (1986). These authors conclude that backscattering and proximity effects are negligible for 100kV Ga^+ beam. At 1.5×10^{-7} C/cm^2 a line pattern with 0.06 µm linewidth was observed.

Adesida et al. (1985) discussed the factors affecting the resolution of ion beam lithography. These considerations led to an estimated minimum linewidth of about 10nm in polymethyl methacrylate (PMMA) using light ions. For gallium this limit is 30 nm.

In a recent study of Morimoto et al. (1987), a field-effect transistor with mushroom gate was fabricated. A mixed exposure of a fine 200keV Be^{++} and a larger 100kV Be^+ focused ion beams was used to get a T-shaped groove in the exposed resist. The average resistance of the 0.25 µm long mushroom gate was 18.5 Ω quite better than the conventional gate resistance of 80.9 Ω.

Different lithographic techniques have been investigated by Morimoto et al (1986): direct-write milling applied to lithography of a bilevel structure, resist exposure using dry development and resist patterning with wet development.

The results demonstrated the practical feasibility of FIB lithography in the 100 nm range. Future developments in 10 nm range and less can seriously be considered for the near future. Exposure times lower than EBL and reduction of proximity effects are important advantages of IBL. Progress in FIB columns reliability could advance the advent of commercial IB maskers.

Micromachining

A lower beam energy (10 kV range) is usually sufficient as previously noticed to optimize the sputtering yield and avoiding creation of deep defects. The application of FIB machining involves VLSI and X-ray mask repair, creation of optical structures in integrated optoelectronic devices, making and breaking connections on conductors. Heavy ions such as gold are suitable to maximize the sputtering yield.

Heard et al. (1985) reported a complete process of mask repair. The opaque defect can be located by scanning ion microscopy (SIM), using topography and atomic number contrast of the secondary electron signal as in SEM. This image, which must be acquired in a time as short as possible to minimize the ion exposure of the mask, is memorized. The precise coordinates of the defect are calculated. The unwanted material is then removed by scanning the ion beam.

A recent paper by Harriott et al. (1987) demonstrates the fabrication of mirror facets in active InP laser devices. In this experiment a 20kV Ga beam is focused in a 0.2µm spot. The probe current is 160pA. The characteristics of the laser before and after machining are reported. The data indicate an increase of lasing threshold of about 5%, a decrease in quantum efficiency of 8 % and little change in light output. The success of the FIB micromachining techique was attributed to shallow beam penetration (about 30nm) due to the low beam energy (20 keV) which avoided most crystal damage in the active region. The milling time necessary for typical faceting is 20 min which limits the development of this technique for mass production.

Demonstration of an operating laser diode with an FIB machined output mirror has been given by Puretz et al (1986). This laser was a Standard V-channel-substrate inner-stripe device. The micromachining was accomplished with a 20kV Ga^+ ion beam of 3×10^{-10} A current. The spot diameter was 0.25 µm. The machining was made by raster scanning the beam in a rectangular pattern along the edge of the laser. Redeposition of sputtered atoms was minimized by starting the beam scan from the cleaved facet into the material. The light output characteristics of the original cleaved facet laser have been maintained by the machining process.

Creation of submicron dimension connections between crossing Al conductors separated by oxide (SiO_2) has been reported by Musil et al. (1986). This technique is based on the redeposition of the sputtered Al of a lower metal layer on the sidewalls between the two Al layer to form a connection. The resistance of these connections is 3 Ω. With simple milling, cuts in 0.65µm thick 10µm wide conductors produced open-circuit resistances > 20 MΩ.

In a following paragraph, we will present our contribution to this domain of application to microcircuits surgery.

Microanalysis

We will discuss briefly this domain which is not specific of microelectronics but which can become one of the best tools for precise chemical analysis of complicated semi-conductor structures. High performance secondary ion mass spectrometers have been used in an increasing

number of domains from metallurgy to biology. To reach submicron analysis after energy and mass selection is impossible with conventional ion sources because of their poor brightness and the subsequent low number of secondary ions collected. The LMIS equipped FIB column built by Levi-Setti's group in Chicago has boosted the resolution of SIMS microanalysis. The authors recently reported 20nm estimated resolution (Levi-Setti et al. 1985). The probe current available (1.6) pA with Ga+ LMIS at this level of resolution approaches the theorical resolution limits of the SIMS method. This is the beginning of a generation of high resolution SIM and SIMS if one considers that the sensitivities are of the same order as those of the best classical instruments with a substantial gain in resolution. This opens new perspectives in submicronic electronic devices characterization.

New Results

We include several new applications to microelectronics of the low energy (20kV) focused ion beam column which we have coupled with a scanning electron microscope.

Electron and ion beams cross on the sample and can be scanned by same or separate signals. The advantage of this system is a precise and easy localization of the area to be machined and real time SEM control of the micromachining process without destroying the sample. We have also the ability to measure the evolution of the electrical properties of the devices during operation. The ion column has been used in the ion mode and droplet mode. Figure 2 shows the complete apparatus. A high vacuum of $1x10^{-7}$ Torr is maintained in the specimen chamber while 200 l/s ion pump maintains $1x10^{-8}$ Torr in the ion column.

Devices characterization

During the numerous steps involved in microcircuit fabrication, some defects can appear because of failures in lift-off, metal deposition, lithographic process, etching. Characterization of devices (FIB microtomy) can be useful to localize and determine the origin of those defects without destroying the complete wafer.

The SEM micrograph of Fig 3a shows interdigitated metal-semiconductor field effect transistors (MESFET) where a trench has been machined with a 15kV Ga beam. Micrographs 3b and 3c are enlarged views of the active region of a transistor. The gate centered between source and drain appears under a transparent polyimide layer. On each side, the gold platinum deposit has spread slightly down the gate recess. In micrograph 3d, an unexpected dark polyimide layer is noticed between the two clear gold (surface) and AuGeNi layers. The strong chemical contrast makes the location of different layers very easy.

In the following device, a failure consists of a poor electrical contact

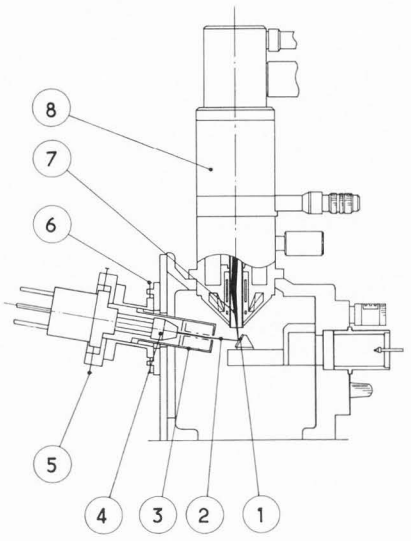

Figure 2 - Coupled FIB-SEM system. 1 - Target. FIB column : 2 - ion beam. 3 - acceptance aperture, lens, stigmator, deflecting plates. 4 - ion gun. 5 - alignment. 6 - E-beam. I-beam crossing adjustment. 5 - E-beam. 8 - SEM.

between a resistor and its connections due to thin (1 to 3 nm) tantalum oxynitride covering the tantalum nitride resistor. As a primary step in the repair process, a 5µm wide and about 2µm deep rectangular well has been machined to characterize metal layers and measure their respective erosion times. Figure 4a is a SEM micrograph of the well walls, displaying stacked layers, the corresponding chemical contrast between the upper 400 nm gold layer (clear), 50 nm titanium (dark) 1 to 3 nm tantalum oxynitride (not resolved), 40 nm tantalum nitride (clear) and lower GaAs substrate (dark) layer is excellent. Then, several rectangular wells were dug, the material erosion being stopped at the tantalum level, after oxide removal (micrograph 4b). The last step for repair consists of bilevel contact restoration with a final localized metal deposition in the wells, either by lithography, or by focused droplet beam (FDB). This last part of the process is underway.

Microcircuit tuning

Using 19.5kV energy, (0.3µm spot, I_{probe} = 50pA) Ga ions, we demonstrated the feasibility to tune passive microdevices. Figure 5a shows the contacts connected for in-situ real time electrical measurements. The resistor is a doped GaAs 10 µm-long and 10 µm-wide

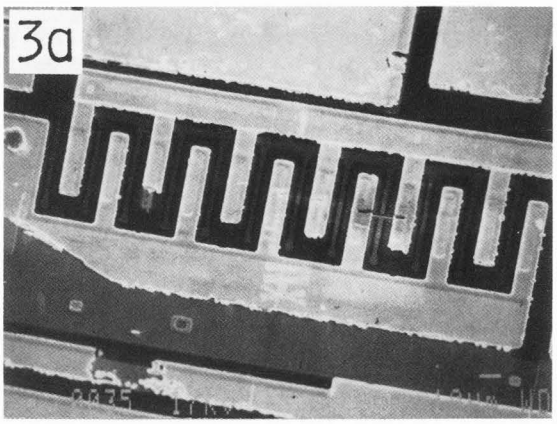

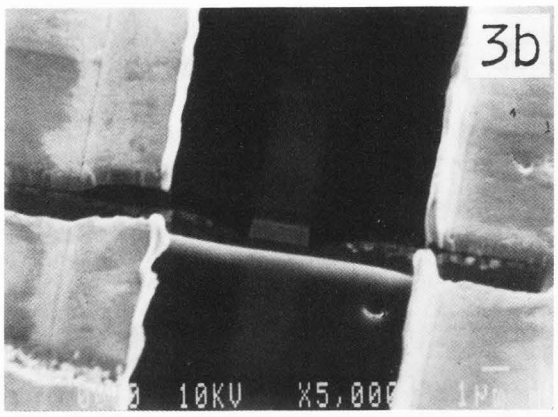

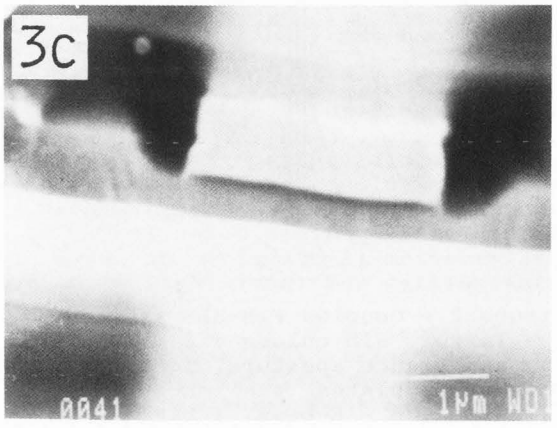

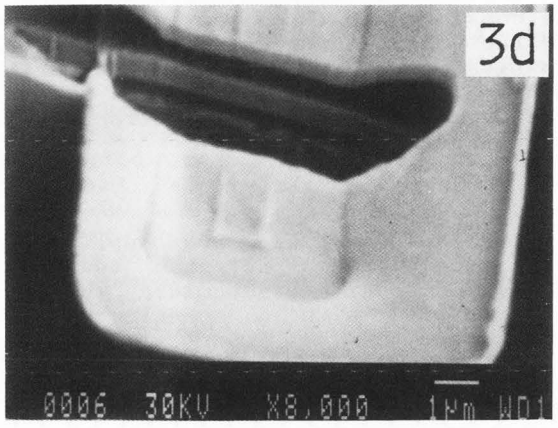

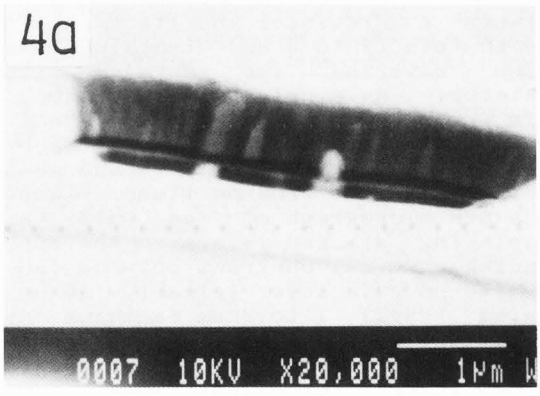

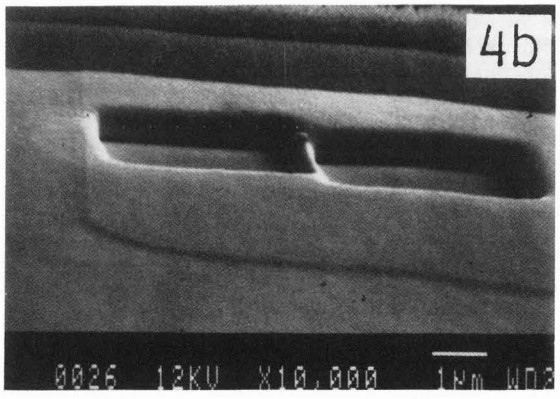

Figure 3 - a) Interdigitated field-effect transistors (MESFET) and a cut dug in the active region.
- b) and c) Magnified views of FET gate.
- d) The polyimide layer is intercalated between the Au(surface) and AuGeNi layers (clear).

Figure 4 - a) Rectangular well displaying the circuit tomography. From top to bottom Au (bright), titanium (dark), tantalum oxinitride (not resolved) and GaAs substrate (dark).
- b) Aspect of the resistor contacts after the first step of the repair. Smooth tantalum nitride surface has been cleared off.

stripe located in proton/boron implanted semi-insulating GaAs. The calculated resistance value is 50 Ω. In fact, the actual value is about 32 Ω. A square well was dug in the resistor to produce a desired increase of resistance. Figure 5b shows the modified resistor. Resistance R stays stable at 50 Ω within less than 0.1 Ω and exhibits a linear I(V) characteristic.

The corresponding 1/R curve 5c versus time is a straight line which suggests a constant sputtering yield if we exclude the very beginning and end of erosion. This can be due respectively to surface impurities or oxides with lower

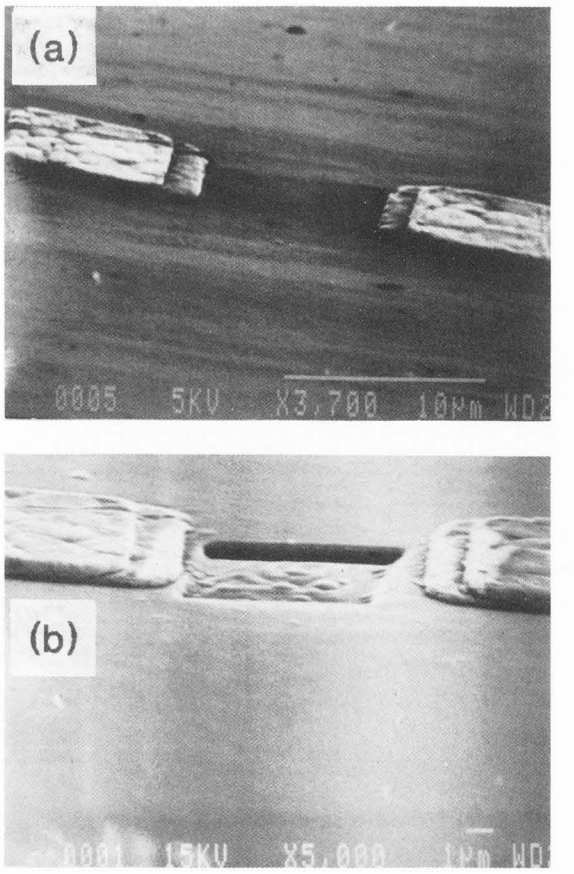

Figure 5 - a) aspect of the implanted resistor before tuning.
- b) tuned resistor R=50 ohms.
- c) 1/R curve versus working time.

sputtering yield and to the fact that after 39 min the beam reached the substrate.

Connection modifications by FIB and FDB

The connection studied for cuts is a gold deposited stripe on H/B amorphized GaAs. Several cuts have been carried out with the Ga^+ ion beam (15kV I_p=30pA). Figure 6 shows the several µm cuts machined in Au layer. A surprising result is

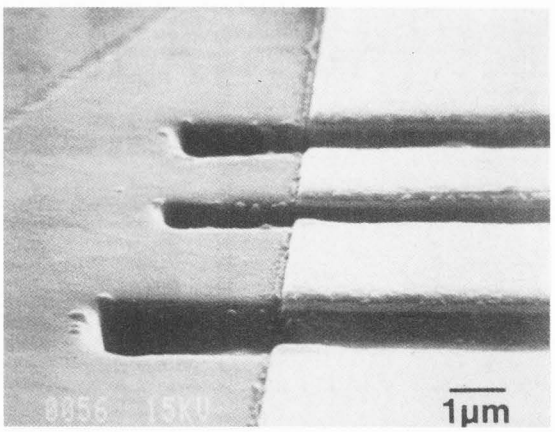

Figure 6 - Several cuts can be seen on the gold stripe. Each one adds 8 kohms to the total resistance.

that each cut adds only 8 kΩ to the total resistance. A subsequent soft chemical etch increases this value to several tens of megohms. This suggests that ion irradiation induces a surface restructuring accompanied by some conductivity. Musil et al. (1986) results demonstrate that this effect does not occur on real insulators.

As previouly noticed, LMIS also produce small charged clusters whose sizes range from some atoms to 0.1 to 1 µm droplets. Droplet and cluster emission have been studied for different metals. Emission characteristics of gold droplet emitters were investigated by D'Cruz et al. (1985) and Papadopoulos et al. (1986). D'Cruz reported a droplet emission angle of only 2-3 ° (instead of 20° in the ion case) for a typical $5x10^5$ $\mu m^3/s/Sr$ flux and $3x10^3$ $\mu m^3/s$ deposition rate at 150 µA. More recently, François et al. (1987) studied the LMIS cluster beam constituents and their role in the properties of unfocused deposited film.

The focusing properties of electrostatic lenses being independent of charge to mass ratio, focusing of charged droplets is theoretically possible in an FIB system. First Mahony et al (1982, 1984) attempted to focus this droplet beam and obtained 60µm wide gold deposited dots. Ben Assayag et al (1986) reported 2.3 µm gold deposited dots in 10s with rates of 1.5 $\mu m^3/s$ using a Au focused droplet beam (FDB). By scanning the metal beam, 100µm long and 4µm wide metallic wires were drawn in 70s.

In order to apply the focused droplet beam technique to microelectronic engineering, a precise characterization of indium cluster emission has been achieved. Figure 7 is a focus series of

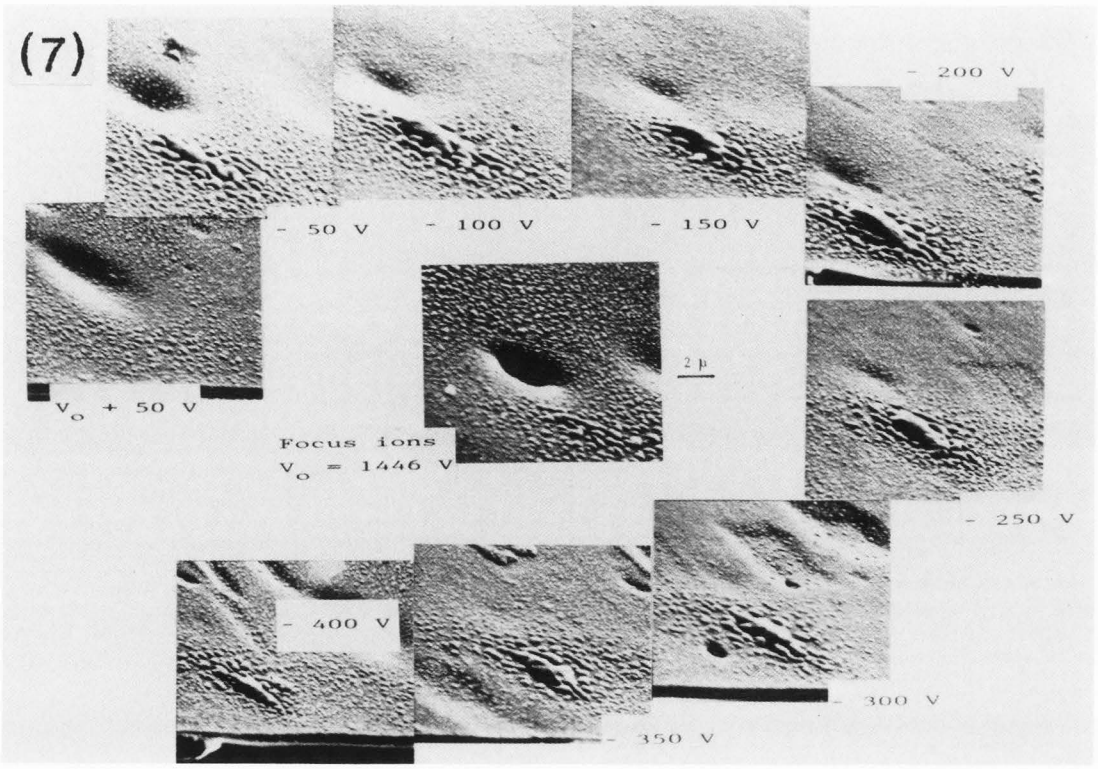

Figure 7 - Indium has been deposited with In focused droplet beam for different lens excitation. The best focus is about 50 to 150 eV excitation below best ion beam focusing (V_{ions}=2kV, V_{lens}=1.4kV, I=30µA).

indium ions and droplets reaching a GaAs surface. Accelerating voltage was close to 2 kV and the extracted current 30 µA. When ions are perfectly focused (V_{lens} = 1400 V) droplets are overfocused, best droplet focus is 100 to 200V below the-lens voltage of the best ion focus. These results confirm that droplets have an energy deficit with respect to ion energy. A rough evaluation by Ben Assayag et al (1986) gave about -350 eV for gold at I = 150 µA. The smallest In deposition dot achieved was 2µm wide in 2 min and for a current I = 30 µA (Figure 8).

Metal deposition by simply scanning a focused droplet beam (FDB) is very attractive because FDB can be done in the same apparatus as FIB by changing the emission current. Application to UV and X mask repair includes clear and opaque defects. To investigate the possibility of directly establishing electrical connections by FDB, we have employed our SEM/FIB system, using the FIB column for FDB. In Figure 9, a previously tuned resistor (R=100 Ω) has been short-circuited with a 3µm-wide metal deposition line. The initial resistance was 100 Ω and the residual value about 4 Ω. This example shows the feasibility of circuit restructuring and repair by the FDB technique.

Conclusion

This review paper has shown that a large number of applications involving focused ion beam techniques has been implemented in microcircuit engineering. Recent developments of higher resolution focused beams increase the perspective of FIB technique to future low dimensional (2, 1 or even 0D) devices. The unique ability to modify devices by software makes the use of FIB very attractive for the creation of exotic circuits. A particularly promising domain of applications is integrated microoptoelectronics where FIBI modifies material properties in the X-Y direction and MBE in the Z-direction.

The weakness of FIB is to be found in the still insufficient current density and consequent low processing speed common to all focused beam systems. The time necessary to expose a unit area of a wafer to obtain a given effect depends on total dose which is much lower than in the case of broad beams in spite of higher current density. We have shown the first results of FDB repair of a circuit. Some efforts remain to be made to make FDB reliable, particularly, one would like to gain better knowledge of the droplet emission mechanism which could be tightly linked with the ion emission process. We should remark that the large energy dispersion of droplet beams (50eV at least) limits resolution more dramatically for FDB than FIB.

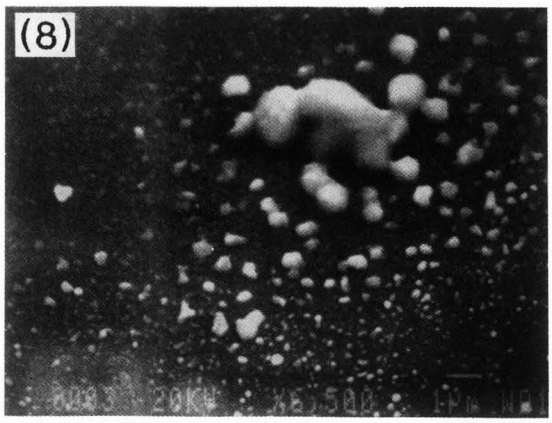

Figure 8 - An In dot was deposited for I=30μA and t=2min.

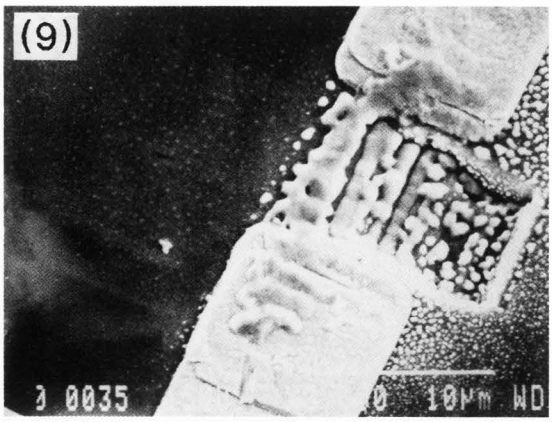

Figure 9 - An FDB deposited Indium line straps the resistor contacts. Residual resistance is 4 ohms.

Acknowledgments

The authors are grateful to J. Gierak for his continuous help in solving all technical problems.

All the work on microcircuit surgery of our group has been made in collaboration with the CNET-Bagneux and specially with the division of M. Bon.

References

Adesida I, Kratschmer E, Wolf ED, Muray A, Isaacson M. (Jan/Feb 1985). Ion beam Lithography at nanometer dimensions. J. Vac. Sci. Technol. B3(1); 45-49.

Andersen HH, Bay HL (1981). Sputtering yield measurements. Sputtering by particles bombardment I. Springer-Verlag Berlin Heidelberg New York. 1984; 169.

Arimoto H, Takamori A, Miyauchi E, Hashimoto H. (1985). Formation of submicron isolation in GaAs by implanting a focused boron ion beam emitted from Pd-Ni-Si-Be-B LM ion source. J. Vac. Sci. Technol. B3(1); 54-57.

Ben Assayag G, Orloff J, Swanson LW. (1986). Focused droplet beam from a gold liquid metal ion source. Journal de physique. Coll. C7, Sup. 11. 47; 389-397.

Ben Assayag G, Sudraud P, Jouffrey B. (1985). In-situ high voltage TEM observation of an electrohydrodynamic (EHD) ion source Ultramicroscopy. 16; 1-8.

Bozack MJ, Swanson LW, Orloff J. (1985). A successful liquid metal ion source : the ideal requirements. Scanning Electron Microsc. 1985; IV: 1339-1345.

Clampitt R, Aitken KL, Jefferies DK. (1975). Abstract : Intense field-emission ion source of liquid metals. J. Vac. Sci. Technol. 12; 1208.

Cleaver JRA, Heard PJ, Ahmed H. (1983). Scanning ion beam lithography with magnetic ion species filter. Microcircuit engineering 83. Ahmed H, Cleaver JRA, Jones GAC (eds). Academic Press. London; 136-142.

Cutler PH, Chung M, Feuchtwang TE, Kazes E. (1986). The effects of gravitational and hydrostatic pressure on the equilibrium shape of a conducting fluid in an electric field : application to liquid metal ion source. Journal de Physique. Coll. C2. Sup. No3. T47; 87-93.

D'Cruz C, Pourrezaei K, Wagner A. (1985). Ion cluster emission and deposition from liquid metal ion source. J. Appl. Phys. 58(7);2724-2730.

Fox T. R., Levi-Setti R., Lam K. (1981). Magnetic-prism analysis of a practical gallium ion probe from a liquid metal source. Proceedings of 28th IFES. Portland OR ; 92-93.

François M, Pourrezaei K, Bahasadri A, Nayak D. (1987). Investigation of the liquid metal ion source cluster beam constituents and their role in the properties of the deposited film. J. Vac. Sci. Technol. B5(1); 178-183.

Gaubi H, Sudraud P, Tence M, Van de Walle J. (1982). Some new results about in-situ TEM observations of the emission region in LMIS. Proc. 29th IFES. Göteborg. Andrén HO. and Nordén H. (eds). Göteborg; 357-362.

Gesley MA, Swanson LW. (1984). Analysis of energy broadening in charged particle beams. Journ. de Phys. coll C9. supp. No12. T. 45; 167-172.

Gomer R. (1979). On the mechanism of liquid metal electron and ion sources. Appl. Phys. 19; 365-375.

Harriott LR, Scotti RE, Cummings KD, Ambrose AF. (1987). Micromachining of optical structures with focused ion beams. J. Vac. Sci. Technol. B5(1); 207-210.

Hashimoto H, Takamori A, Arimoto H, Morita T, Miayauchi E. (1986). Focused ion beam doping for GaAs MBE growth. Microcircuit Engeneering 4; 181-193.

Heard PJ, Cleaver JRA, Ahmed H. (1985). Application of a focused ion beam system to defect repair of VLSI masks. J. Vac. Sci. Technol. B3(1); 87-90.

Hirayama Y, Suzuki Y, Tarucha S, Okamoto H. (1985). Compositional disordering of GaAs-$Al_xGa_{1-x}As$ superlattice by Ga focused ion beam implantation and its application to submicron structure fabrication. Jap. Jour. of Appl. Phys. 24. No7; 516-518.

Ishida K, Takamori T, Matsui K, Fukunuga T, Morita T, Miyauchi E, Hashimoto H, Nakashima H. (1986). Fabrication of index-guided AlGaAs MQW lasers by selective disordering using Be focused ion beam implantation. Jap. Jour. of Appl. Phys. 25. No9; 783-785.

Karapiperis L, Adesida I, Lee CA, Wolf ED. (1981). Ion beam exposure profiles in PMMA-computer simulation. J. Vac. Sci. Technol. 19(4); 1259-1263.

Karapiperis L, Dubreuil D, David Ph, Dieumegarde D. (1985). Ion Beam lithography : An investigation of resolution limits and sensitivities of ion-beam exposed PMMA. J. Vac. Sci. Technol. B3(1); 353-357.

Komuro M, Kanayama T, Hiroshima H, Tanoue H. (1983). Measurement of virtual crossover in liquid gallium ion source. Appl. Phys. Lett. 42(10); 908-910.

Krohn VE. (1961). Liquid metal droplets for heavy particle propulsion. Prog. in Astro. and Rocketry. 5: 73-80.

Krohn VE, Ringo GR.(1975). Ion source of high brightness using liquid metal. Appl. Phys. Lett. 27; 479-481.

Levi-Setti R, Crow G, Wang YL. (1985). Progress in high resolution scanning ion microscopy and secondary ion mass spectrometry imaging microanalysis. Scanning Electron Microsc. 1985; II: 535-551.

Mahoney JF, Yahiku AY, Daley HL, Moore RD, Perel J. (1969). Electrodynamic source. J. Appl. Phys. 40; 5101-5105.

Mahony C, Gowland L, Prewett PD. (1982). Liquid metal field emission systems for high technology applications : The FED sprayer. 29th IFES Göteborg. Andrén HO. and Nordén H. (eds). Göteborg; 383-390.

Mahony C, Prewett PD. (1984). Field emission deposition : ion assisted deposition using liquid metal ion source. Vacuum. 34. No1-2; 301-304.

Mair GLR, Mulvey T. (1984). High brightness sources for electron and ion beam microscopy and micro-lithography. Ultramicroscopy. 15; 255-260.

Mair GLR, Mulvey T. (1985). Liquid metal ion microscopy and secondary ion mass spectrometry. Scanning Electron Microsc. 1985; III: 959-971.

Matsui S, Mori K, Saigo K, Shiokawa T, Toyoda K, Namba S. (1986). Lithographic approach for 100 nm fabrication by focused ion beam. J. Vac. Sci. Technol. B4(4); 845-849.

Miyauchi E, Arimoto H, Bamba Y, Takamori A, Hashimoto H, Utsumi T, (1983). Lateral spread of Be and Si in GaAs implanted with a maskless ion implantation system. Jap. Jour. of Appl. Phys. 22. VII: L423-L425.

Miyauchi E, Hashimoto H. (1986). Application of focused ion beam technology to maskless ion implantation in a molecular beam epitaxy grown GaAs or AlGaAs epitaxial layer for three-dimensional pattern doping crystal growth. J. Vac. Sci. Technol. A4(3); 933-938.

Morimoto H, Onoda H, Sasaki Y, Mitsui Y, Ishiara O, Kato T. (1987). A GaAs metal-semiconductor field-effect transistor with mushroom gate fabricated by mixed exposure of focused ion beams. J. Vac. Sci. Technol. B5(1); 211-214.

Morimoto H, Sasaki Y, Saitho K, Watakabe Y, Kato T. (1986). Focused ion beam lithography and its application to submicron devices. Microcircuit Engineering 4; 163-179.

Moriya S, Komatsu K, Harada K, Kitayama T. (1983). A large angle electrostatic deflection, variable shaped, electron beam exposure system. J. Vac. Sci. Technol. B1(4); 990-994.

Munro J. (1973). Computer-aided design of electron lenses by finite element method. In: Image processing and computer-aided design in electron optics. Hawkes PW. (Ed) Academic Press. London; 284-323.

Musil CR, Bartelt JL, Melngailis J. (1986) Focused ion beam microsurgery for electronics IEEE electron device letters. EDL-7. N°5; 285-287.

Nakamura K, Nozaki T, Shiokawa T, Toyoda K, Namba S. (1987). Formation of submicron isolation in GaAs by Ga focused ion beam implantation. J. Vac. Sci. Technol. B5(1); 203-206.

Ochiai Y, Gamo K, Namba S. (1984). Pressure and irradiation angle dependence of maskless ion beam assisted etching of GaAs and Si. Jour. Vac. Sci. Technol. B3(1); 67-70.

Ohana R. (1980). Investigations of the realization and of the properties of liquid metal ion sources. Thèse de Docteur-ingénieur. Orsay.

Orloff J, Sudraud P. (1985). Design of a 100 kV, High resolution focused ion beam column with a liquid metal ion source. Microcircuit Engineering. 3; 161-165.

Pang SW, Lyszczarz TM, Chen CL, Donnelly JP, Randall JN. (1987). Masked ion beam lithography for submicrometer-gate-length transistors. J. Vac. Sci. Technol. B5(1); 215-218.

Papadopoulos S, Barr DL, Brown WL. (1986). On the energy distribution of clusters from liquid gold ion sources. Journal de Physique. Coll. C2, Supp. 3, 47; 101-106.

Puretz J, DeFreez RK, Elliott RA, Orloff J. (1986). Focused-ion-beam micromachined AlGaAs semiconductor laser mirrors. Electronic Lett. 22, 13; 700-701.

Reuss RH, Morgan D, Greeneich EW, Clark Jr WM, Rench DB. (1985). Vertical npn transistors by maskless boron implantation. J. Vac. Sci. Technol. B3(1); 62-66.

Shiokawa T, Kim PH, Toyoda K, Namba S, Gamo K, Aihara R, Anazawa N. (1985). 200 kV Mass-separated fine focused ion beam apparatus. Jap. J. of Appli. Phys. 24. VII; 566-568.

Sigmund P. (1981). Sputtering by ion bombardment : Theoretical concepts. Sputtering by particle bombardment I. Topics in Applied physics, V 47, Springer-Verlag, Berlin; 9-71.

Slingerland HN. (1984). Optimization of a chromatically limited ion probe. Microcircuit Engineering. 2. No4; 217-226.

Sudraud P. (1979). Field emission mechanisms responsible for charged particle emission from a surface and elaboration of a high brightness ion source. Thèse d'Etat. Orsay; 126.

Sudraud P, Orloff J, Ben Assayag G. (1986). The effect of carbon bearing gases and secondary electron bombardment on a liquid metal ion source. Jour. de Phys. Coll C7. Supp. 11. 47; 381-387.

Swanson LW, Kingham DR. (1986). On the mechanism of liquid metal ion source. Appl. Phys. 41; A: 223-232.

Taylor GI. (1964). Disintegration of water drops in an electric field. Proc. Roy. Soc. Lon. A280; 383-397.

Townsend P D, Kelly JC, Hartley NEW. (1976). Ion implantation, sputtering and their applications. Academic Press. New York ch.4; 65-87.

Ward JW. (1985). A Monte Carlo calculation of the virtual source size for a liquid metal ion source. J. Vac. Sci. Technol. B3(1); 207-213.

Wilson R G, Brewer G R. (1979). Ion beams with applications to ion implantation. Krieger R. E. (ed) New York 1979; 357-398.

Discussion with Reviewers

D.McPhail: The authors suggest that focused ion beams may in future be used to image materials such as low dimensional structures. This may require beams focused down to ten nm or less. What are the prospects of this and to what extent will natural straggling associated with the collision cascade then limit the lateral resolution? How does the lateral straggling vary in semiconducting materials such as GaAs, with the mass and the energy of imaging species, upon its angle of incidence, and upon the target density?

Authors: Scanning ion microscopy can theoretically offer ultimate resolution as small as SEM, or smaller: Levi-Setti et al (1985) reported the feasibility of a probe as small as 20 nm. The limit is linked with the gaussian radius of the source (about 30 to 50nm), due to coulombian interactions near the emissive area. Nanometric probes can only be achieved with more sophisticated optical designs as Köehler illumination. Concerning the **visualization** of low dimensional structures, we think that high resolution SEM is more appropriate. The limits of resolution for **the fabrication** of very small systems as quantum devices by FIB implantation is lateral straggling which enlarges the profile of impurities and the creation of damages in the crystal. Light dopants exhibit larger straggling than heavier ones. The absolute value of the straggling increases with the energy. For GaAs, typical values of straggling are for Si ions 6.5 nm, at 10 keV and 33 nm at 100 keV. (See e.g. Wilson and Brewer 1979).

L.W. Swanson: The authors suggest that the focused beam current density profile is "roughly gaussian". Several workers in this field have recently reported "long tails in the current density distribution for ions such as B^+ and Si^+. Because of such long tails do the authors believe this may limit the usefulness of FIB for localized implantation applications?

Authors: This is a very important remark. The "long tails" observed, especially for singly charged ions are of course transferred into the probe current profile via the chromatic aberration coefficients. This effect seems of very small importance for SIM or for micromachining applications (the strong increase of sputtering yield with incidence is a factor which tends to compensate for this effect). However, the spread of doping due to the presence of "tails" will constitute a limitation for highly localized implantation if its width is comparable with the expected straggling.